Electronic Supplementary Material (ESI) for Dalton Transactions
This journal is © The Royal Society of Chemistry 2013

Electronic Supplementary Information

Strategically modified FRET based tri-color emissive rhodamine-pyrene conjugate as Al^{3+} selective colorimetric and fluorescence sensor for living cell imaging

Animesh Sahana,[a] Arnab Banerjee,[a] Sisir Lohar,[a] Avishek Banik,[b] Subhra Kanti Mukhopadhyay,[b] Damir A. Safin,*[c] Maria G. Babashkina,[c] Michael Bolte,[d] Yann Garcia*[c] and Debasis Das*[a]

[a]*Department of Chemistry, The University of Burdwan, 713104, Burdwan, West Bengal, India. Fax: (+91) 342 2530452; E-mail: ddas100in@yahoo.com*

[b]*Department of Microbiology, The University of Burdwan, 713104, Burdwan, West Bengal, India.*

[c]*Institute of Condensed Matter and Nanosciences, Molecules, Solids and Reactivity (IMCN/MOST), Université Catholique de Louvain, Place L. Pasteur 1, 1348 Louvain-la-Neuve, Belgium. Fax: +32(0) 1047 2330; Tel: +32(0) 1047 2831; E-mail: damir.safin@ksu.ru, yann.garcia@uclouvain.be*

[d]*Institut für Anorganische Chemie J.-W.-Goethe-Universität, Frankfurt/Main, Germany.*

Materials and methods. High-purity HEPES, rhodamine B, pyrene aldehyde, and ethylenediamine were purchased from Sigma Aldrich (India). $Al(NO_3)_3 \cdot 9H_2O$ was purchased from Merck (India). Solvents used were of spectroscopic grade. Other chemicals were of analytical reagent grade and had been used without further purification except when specified. Mili-Q Milipore® 18.2 MΩ cm^{-1} water was used throughout all the experiments. *N*-(rhodamine-B)lactam-ethylenediamine was prepared according to the literature mothod.[1] IR spectra in KBr were recorded on a JASCO FTIR-H20 spectrometer. ^1H NMR spectra in DMSO-d_6 were recorded with a Bruker Advance 300 MHz using tetramethylsilane as an internal standard. Absorption spectra were recorded with a JASCO V-570 spectrophotometer. Mass spectra were performed on a QTOF Micro YA 263 mass spectrometer in ES positive mode. All pH measurements were performed with Systronics digital pH meter (model 335). Fluorescence spectra were recorded with a Hitachi F-4500 spectrofluorimeter. Time-resolved fluorescence life time measurements were performed using a picosecond pulsed diode laser-based time-correlated single photon counting (TCSPC) spectrometer from IBH (UK) at λ_{ex} = 375 nm and MCP-PMT as a detector. Emission from the sample was collected at a right angle to the direction of the excitation beam maintaining magic angle polarization (54.71). The full width at half maximum (FWHM) of the instrument response function was 250 ps and the resolution was 28 ps per channel. The data were fitted to multi exponential functions after deconvolution of the instrument response function by an iterative reconvolution technique using the IBH DAS 6.2 data analysis software in which reduced w2 and weighted residuals serve as parameters for goodness of fit. Elemental analysis was performed using Perkin Elmer CHN-Analyzer.

This journal is © The Royal Society of Chemistry 2013

Imaging system. The imaging system is composed of an inverted fluorescence microscope (Leica DM 1000 LED), digital compact camera (Leica DFC 420C), and an image processor (Leica Application Suite v3.3.0). The microscope is equipped with a mercury 50 W lamp.

Preparation of cells. Pollen grains were obtained from freshly collected mature buds of *Allamanda puberula* (Aapocynaceae), a common ornamental plant with bell shaped bright yellow flower by crashing stamens on a sterile petriplate and suspending them in normal saline. After crashing the stamen, debrishes are removed by filtering through a thin layer of non absorbant cotton and the suspended pollens are collected by centrifugation at 5000 rpm for five minutes. The pollen pellet was then washed twice in normal saline and then incubated in a solution of $Al(NO_3)_3 \cdot 9H_2O$ (0.1 mg/mL) for 0.5 h at ambient temperature. After incubation they are again washed in normal saline as mentioned above and then photographed under various objectives using UV filter in a LEICA Fluorescence microscope in presence and absence of the ligand. Both Al^{3+} treated and untreated cells were stained with **L** and observed under fluorescence microscope.

UV-Vis and fluorescence titration. The path length of cells used for absorption and emission studies was 1 cm. For UV-vis and fluorescence titrations, stock solution of **L** was prepared (10 μM) in EtOH: H_2O (4:1 v/v) HEPES (0.1 M) buffer. Working solutions of **L** and Al^{3+} were prepared from their respective stock solutions. Fluorescence measurements were performed using 5 nm × 5 nm slit width. Except time dependent spectra, all the fluorescence and absorbance spectra were taken after 0.5 h of mixing of Al^{3+} with **L**.

Quantum yield measurements. The fluorescence quantum yields were determined using Anthracene as a reference with a known ϕ_R value of 0.27 in EtOH.[2] The area of the emission spectrum was integrated using the software available in the instrument and the quantum yield was calculated according to the following equation:[3]

$$\phi_S/\phi_R = [A_S/A_R] \times [(Abs)_R/(Abs)_S] \times [\eta_S^2/\eta_R^2],$$

where ϕ_S and ϕ_R are the fluorescence quantum yield of the sample and reference, respectively; A_S and A_R are the area under the fluorescence spectra of the sample and the reference, respectively; $(Abs)_S$ and $(Abs)_R$ are the corresponding optical densities of the sample and the reference solution at the wavelength of excitation; η_S and η_R are the refractive index of the sample and reference, respectively.[3]

Job's plot from fluorescence experiment. A series of solutions, containing **L** and $Al(NO_3)_3 \cdot 9H_2O$ were prepared such that the total concentration of Al^{3+} and **L** remained constant (10 μM) in all the sets. The mole fraction of **L** was varied from 0.1 to 0.9. The fluorescence intensity at 586 nm was plotted against the mole fraction of **L** in solution.

Synthesis of (*E*)-3',6'-bis(diethylamino)-2-(2-(pyren-4-ylmethyleneamino)ethyl)spiro[isoindoline-1,9'-xanthen]-3-one (L). A portion of *N*-(rhodamine-B)lactam-ethylenediamine (1.0 g, 2.06 mmol) and pyrene-4-

carbaldehyde (0.4739 mg, 2.06 mmol) were dissolved in freshly distilled EtOH (30 mL). The reaction solution was refluxed for 24 h and stirred for another 2 h at room temperature to form yellow crystals. The crystals were filtrated, washed with ethanol three times. Yield: 91%. M. p. 242 ^{o}C (± 4^{o}C). FTIR (Figure S24 in the Supporting Information), *v*: 1117 (COC), 1634 (C=N), 1684 (C=O) cm^{-1}. ^{1}H NMR, δ: 1.04 (t, $^{3}J_{H,H}$ = 7.0 Hz, 12H, CH_3, Et), 3.26 (q, $^{3}J_{H,H}$ = 7.0 Hz, 8H, CH_2, Et), 3.43 (t, $^{3}J_{H,H}$ = 7.0 Hz, 2H, CH_2, NCH_2CH_2N), 3.57 (t, $^{3}J_{H,H}$ = 7.0 Hz, 2H, CH_2, NCH_2CH_2N), 6.26–6.44 (m, 6H, C_6H_3), 6.99–7.11 (m, 1H, C_6H_4), 7.45–7.58 (m, 1H, C_6H_4), 7.78–7.88 (m, 1H, C_6H_4), 8.06–8.45 (m, 6H, pyrene), 8.93 (s, 1H, pyrene), 8.96 (s, 1H, CHN) ppm. QTOF-MS ES^{+}, *m*/*z* (*I*%): 697.13 (100) $[M + H]^{+}$, 719.14 (22) $[M + Na]^{+}$. *Anal*. Calc. for $C_{47}H_{44}N_4O_2$ (696.89): C 81.00, H 6.36, N 8.04. Found: C 81.47, H 6.21, N 8.13%.

X-Ray crystallography. X-ray data of **L** were collected at 173(2) K on a STOE IPDS-II diffractometer with graphite-monochromatised Mo-K_α radiation generated by a fine-focus X-ray tube operated at 50 kV and 40 mA. The reflections of the images were indexed, integrated and scaled using the X-Area data reduction package.[4] Data were corrected for absorption using the PLATON program.[5] The structure was solved by a direct method using the SHELXS-97 program[6] and refined first isotropically and then anisotropically using SHELXL-97.[6] Hydrogen atoms were revealed from $\Delta\rho$ maps and those bonded to C were refined using appropriate riding models. The hydrogen atom bonded to N was freely refined. Figures were generated using the Mercury program.[7] $C_{47}H_{44}N_4O_2$, M_r = 696.86 g mol^{-1}, monolinic, space group *C*2/*c*, *a* = 23.9547(15), *b* = 8.7450(4), *c* = 36.317(2) Å, β = 103.866(4)°, *V* = 7386.1(7) Å^3, *Z* = 8, ρ = 1.253 g cm^{-3}, μ(Mo-Kα) = 0.077 mm^{-1}, reflections: 27422 collected, 6510 unique, R_{int} = 0.1195, R_1(all) = 0.1306, wR_2(all) = 0.1970.

CCDC 848216 contains the supplementary crystallographic data. These data can be obtained free of charge via http://www.ccdc.cam.ac.uk/conts/retrieving.html, or from the Cambridge Crystallographic Data Centre, 12 Union Road, Cambridge CB2 1EZ, UK; fax: (+44) 1223-336-033; or e-mail: deposit@ccdc.cam.ac.uk.

References

1 J. S. Wu, I.-C. Hwang, K. S. Kim and J. S. Kim, *Org Lett*., 2007, **9**, 907.

2 W. H. Melhuish *J. Phys. Chem.*, 1961, **65**, 229.

3 E. Austin, and M. Gouterman, *Bioinorg. Chem.*, 1978, **9**, 281.

4 Stoe and Cie. X-AREA. Area-Detector Control and Integration Software. Stoe & Cie, Darmstadt, Germany, 2001.

5 A. L. Spek, *Acta Crystallogr.*, 2009, **D65**, 148.

6 G. M. Sheldrick, *Acta Crystallogr.*, 2008, **A64**, 112.

7 I. J. Bruno, J. C. Cole, P. R. Edgington, M. Kessler, C. F.Macrae, P. McCabe, J. Pearson and R. Taylor, *Acta Crystallogr.*, 2002, **B58**, 389.

This journal is © The Royal Society of Chemistry 2013

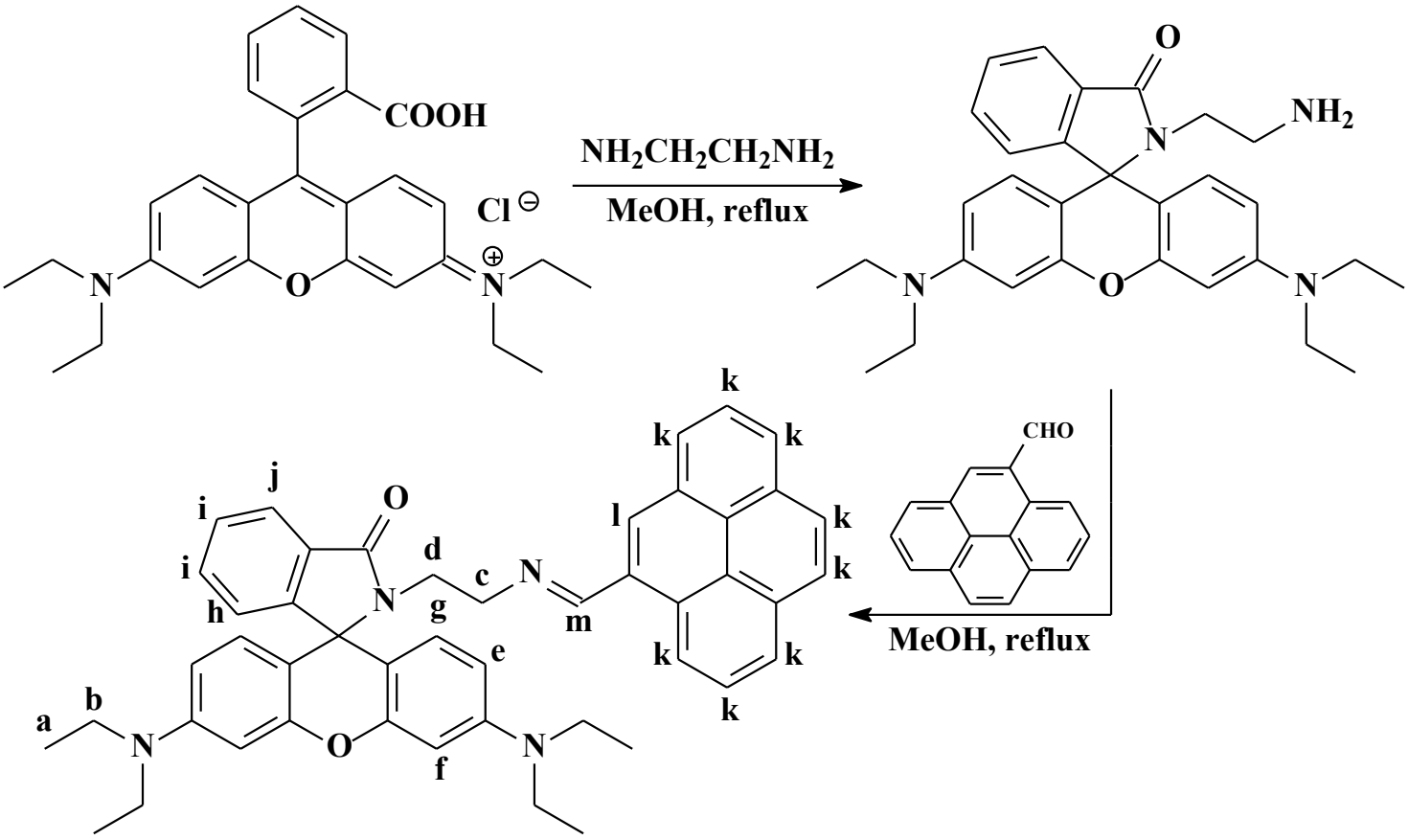

Scheme S1. Synthesis of **L**

This journal is © The Royal Society of Chemistry 2013

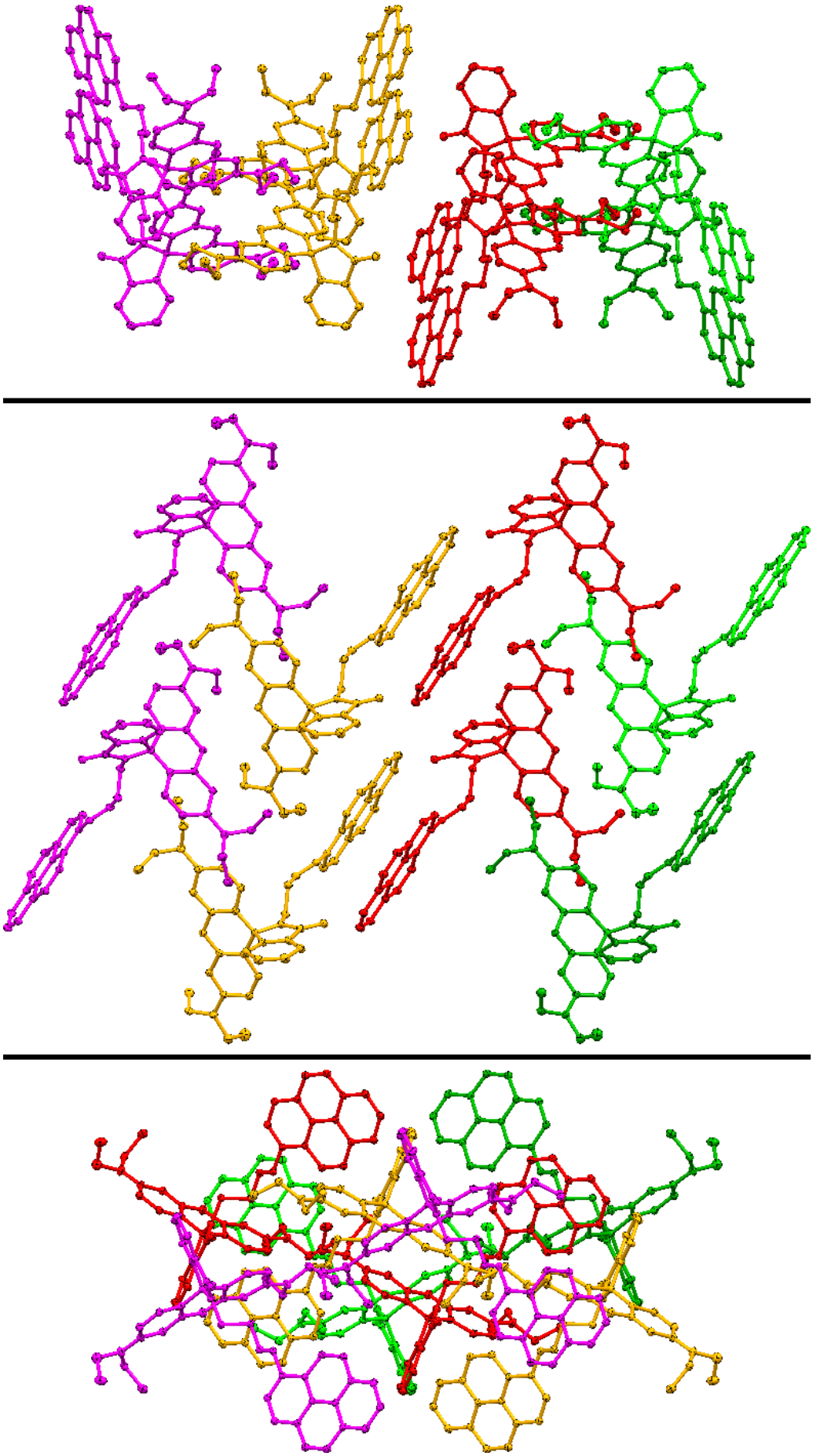

Fig. S1. Crystal structure and packing of **L** along the *0a* (top), *0b* (middle) and *0c* (bottom) axes (bottom; molecules are coloured by symmetry operation). H-atoms were omitted.

This journal is © The Royal Society of Chemistry 2013

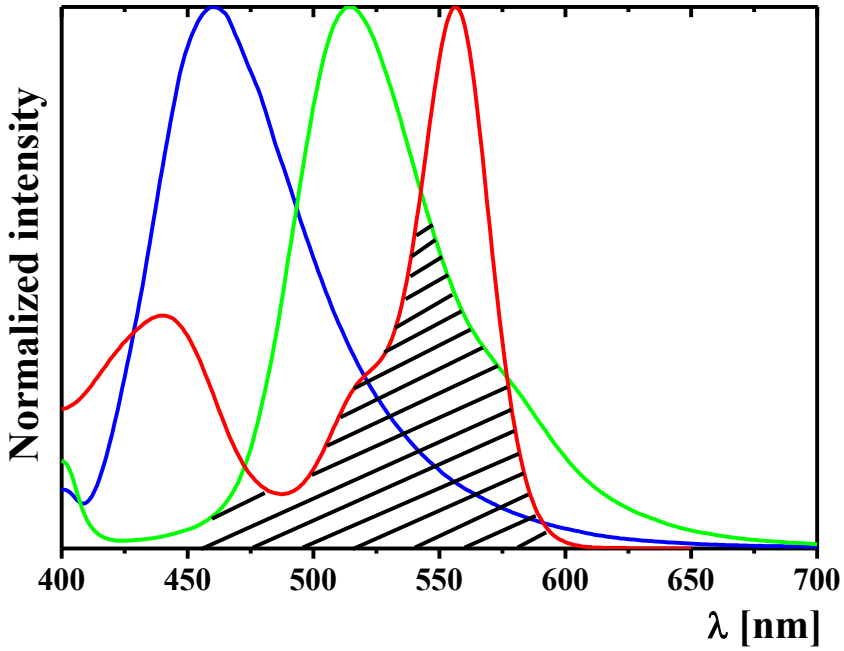

Fig. S2. Emission spectra of **L** (10 μM) (blue), [**L** (10 μM)–Al^{3+} (120 μM)] after 2 min of mixing (green) and absorption spectrum of [**L** (10 μM)–Al^{3+} (120 μM)] after 30 min of mixing (red). The shaded area represents the overlap region of the emission and absorption of the [**L**–Al^{3+}] system, λ_{ex} = 400 nm.

This journal is © The Royal Society of Chemistry 2013

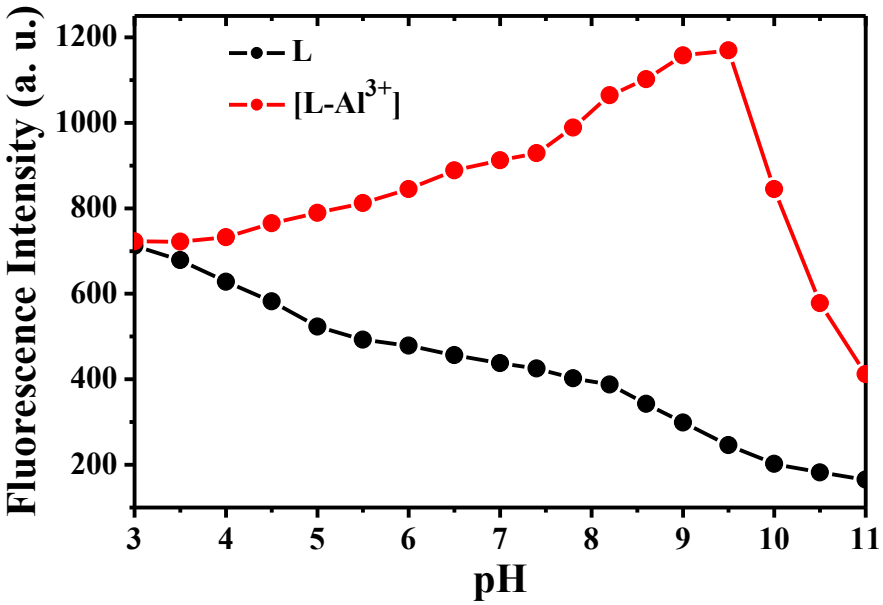

Fig. S3. Effect of pH on the emission intensity of **L** (10 μM) and **L** (10 μM) + Al^{3+} (100 μM) (λ_{em} = 586 nm). All spectra were recorded after 30 min of mixing of **L** with Al^{3+}, λ_{ex} = 400 nm.

This journal is © The Royal Society of Chemistry 2013

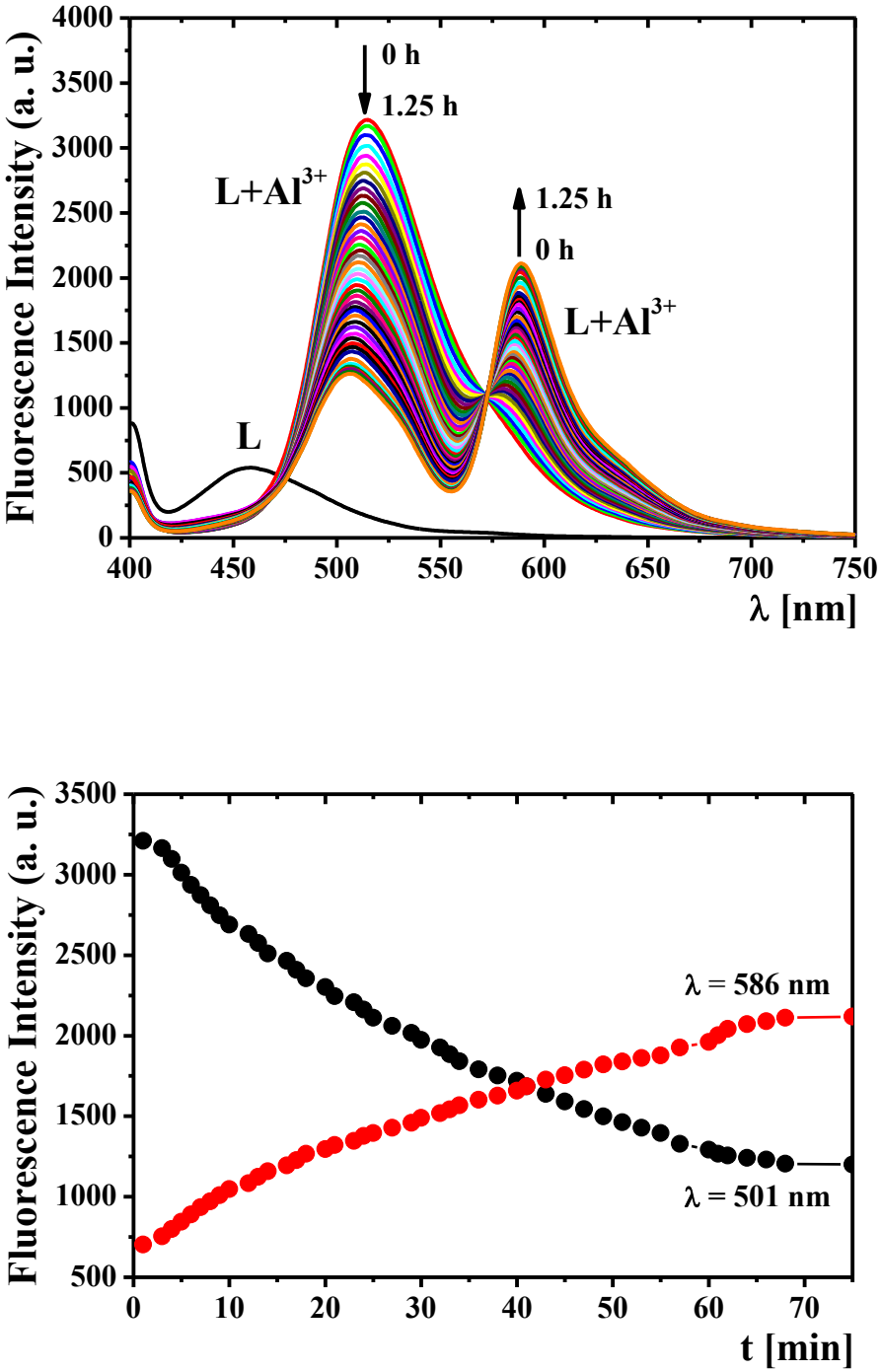

Fig. S4. Time-dependent changes in the emission spectra of **L** (20 μM) after addition of Al^{3+} (100 μM) in HEPES buffer (0.1 M; EtOH:H_2O, 4:1 v/v; pH 7.4; λ_{ex} = 400 nm) (top). Plot of the emission intensities at 586 and 501 nm *vs.* time (bottom).

This journal is © The Royal Society of Chemistry 2013

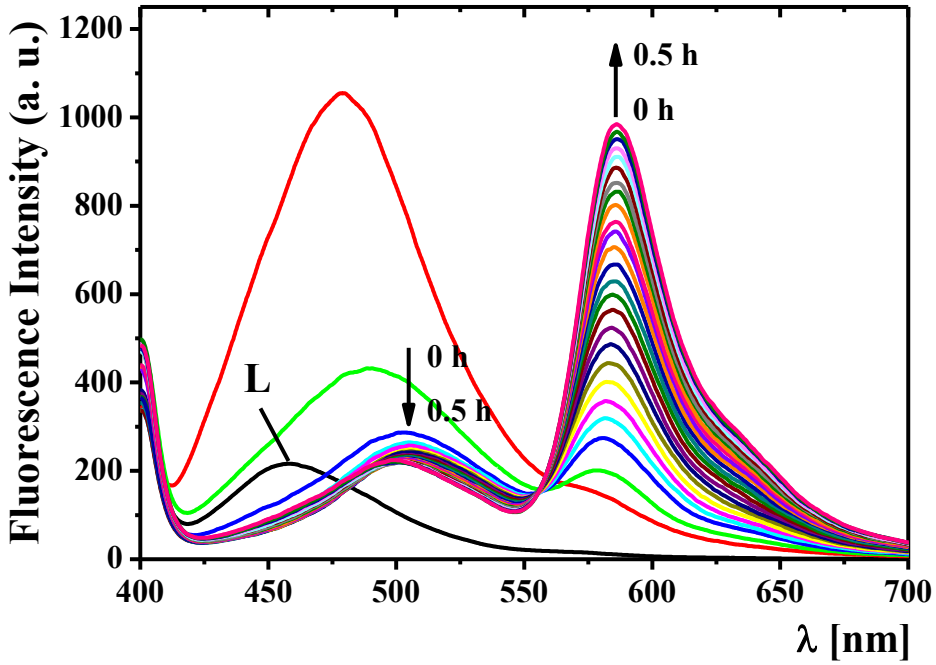

Fig. S5. Emission intensity of **L** (5 μM) in the presence of Al^{3+} (100 μM) as a function of time (from 0 to 0.5 h) in HEPES buffered (0.1 M; EtOH: H_2O, 4:1 v/v; pH 7.4; λ_{ex} = 400 nm) solution.

This journal is © The Royal Society of Chemistry 2013

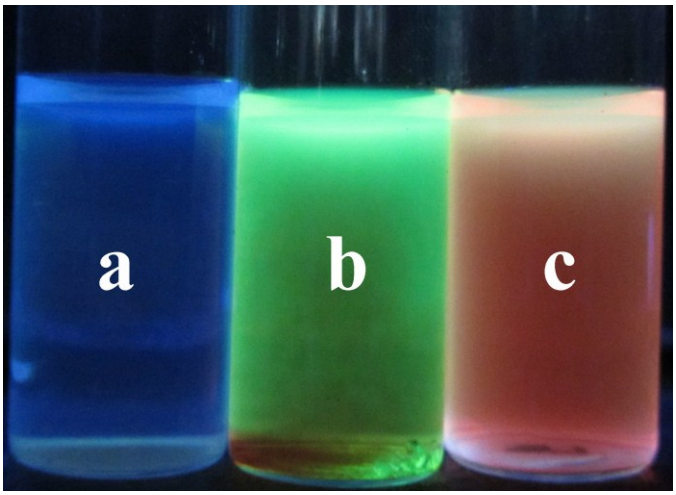

Fig. S6. Al^{3+} induced emission color changes of **L** in EtOH: H_2O (4:1, v/v) as a function of time under a hand held UV lamp: a) **L** (10 μM), b) **L** (10 μM) + Al^{3+} (120 μM) after 5 minutes, c) **L** (10 μM) + Al^{3+} (120 μM) after 20 minutes.

This journal is © The Royal Society of Chemistry 2013

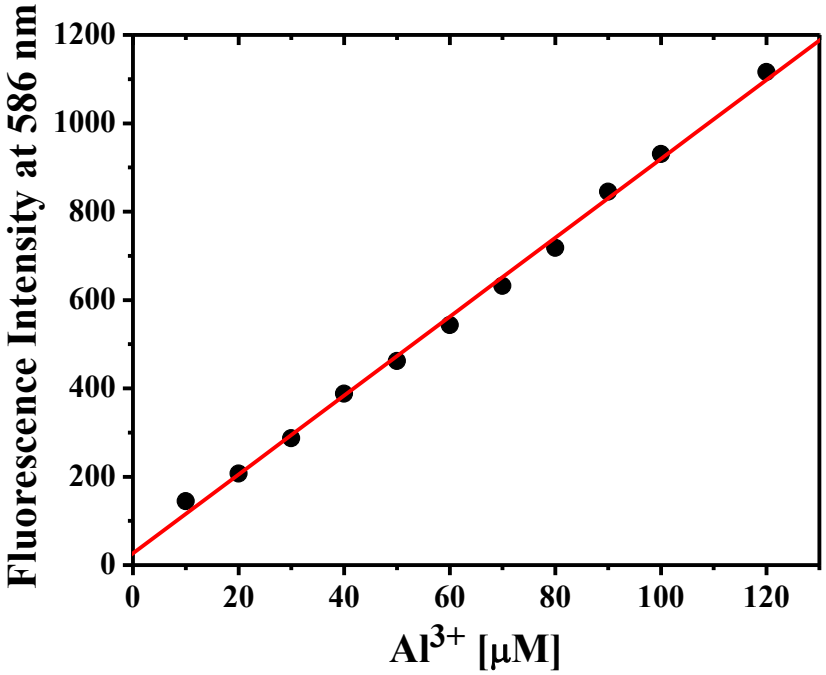

Fig. S7. Plot of the fluorescence intensity of **L** (10 μM) at 586 nm as a function of externally added Al^{3+} (10–110 μM). All spectra were recorded after 30 min of mixing of **L** with Al^{3+}, λ_{ex} = 400 nm.

This journal is © The Royal Society of Chemistry 2013

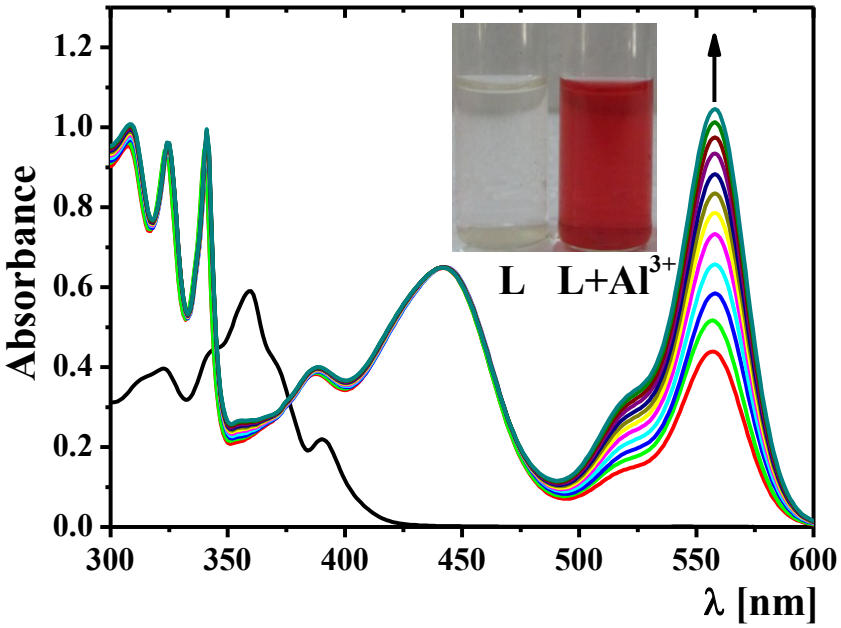

Fig. S8. Changes of absorbance of **L** (10 μM) in HEPES buffered (0.1 M; EtOH: H_2O, 4:1 v/v; pH 7.4) solution upon gradual addition of Al^{3+} (0, 10, 20, 30, 40, 50, 60, 70, 80, 90, 100, 110, 120 μM). Inset shows the naked eye detection of **L** (10 μM) and **L** (10 μM) + Al^{3+} (120 μM). All spectra were recorded after 30 min of mixing of **L** with Al^{3+}.

This journal is © The Royal Society of Chemistry 2013

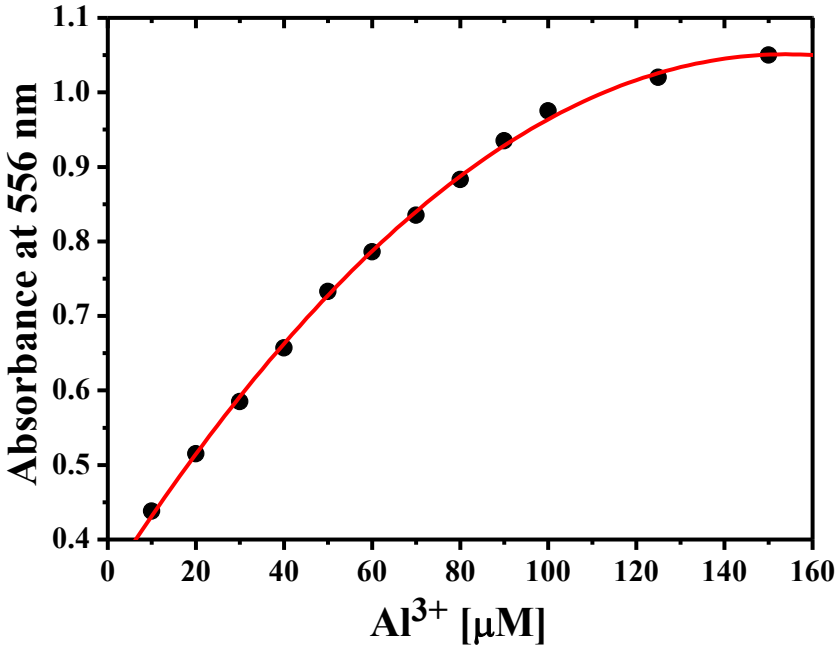

Fig. S9. Plot of absorbance at 556 nm of **L** (10 μM) as a function of externally added Al^{3+} (10–150 μM). All spectra were recorded after 30 min of mixing of **L** with Al^{3+}.

This journal is © The Royal Society of Chemistry 2013

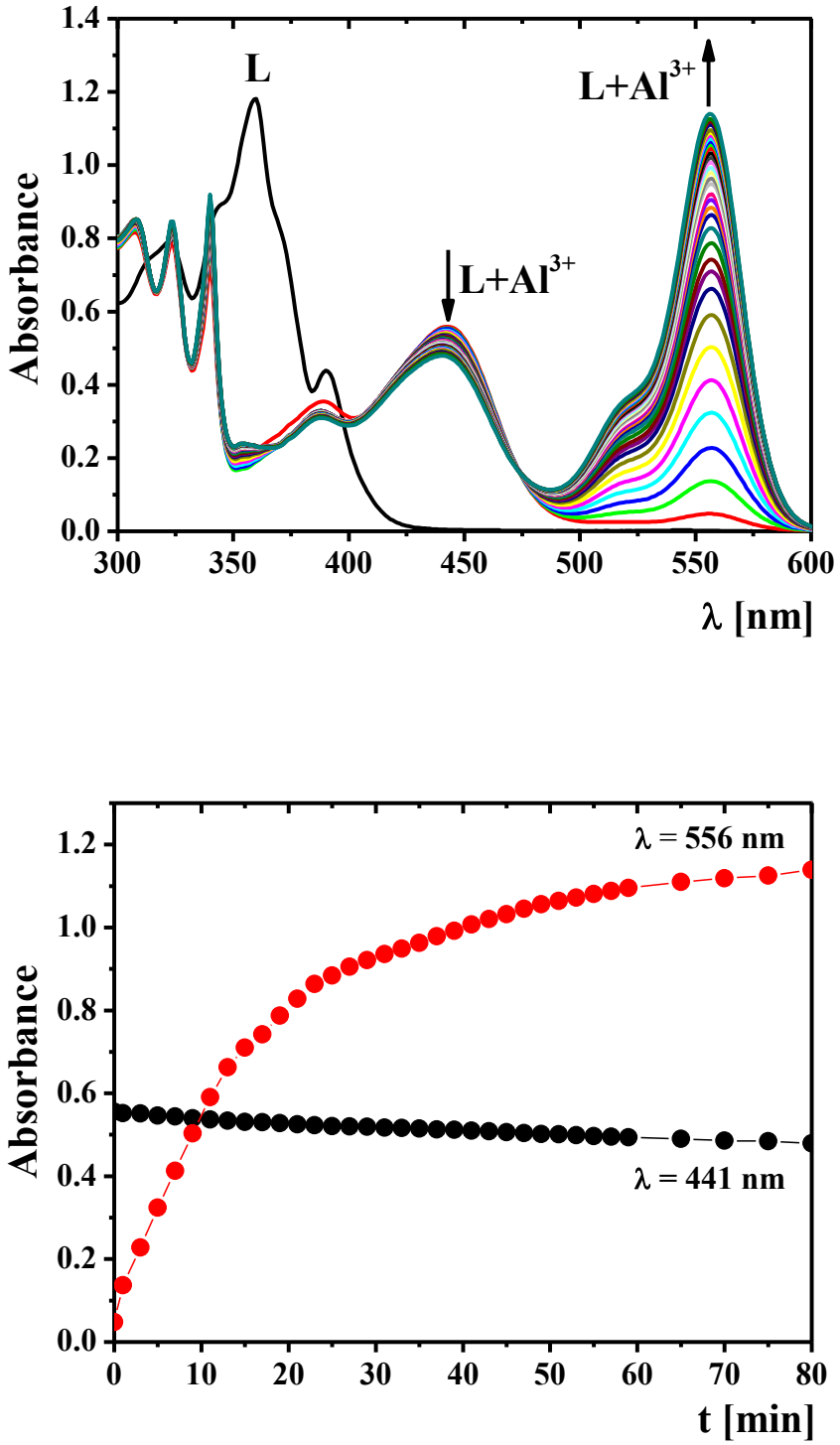

Fig. S10. Time-dependent changes in the absorption spectra of **L** (20 μM) after addition of Al^{3+} (100 μM) in HEPES buffer (0.1 M; EtOH:H_2O, 4:1 v/v; pH 7.4) (top). Plot of the absorbance intensities at 556 and 441 nm *vs.* time (bottom).

This journal is © The Royal Society of Chemistry 2013

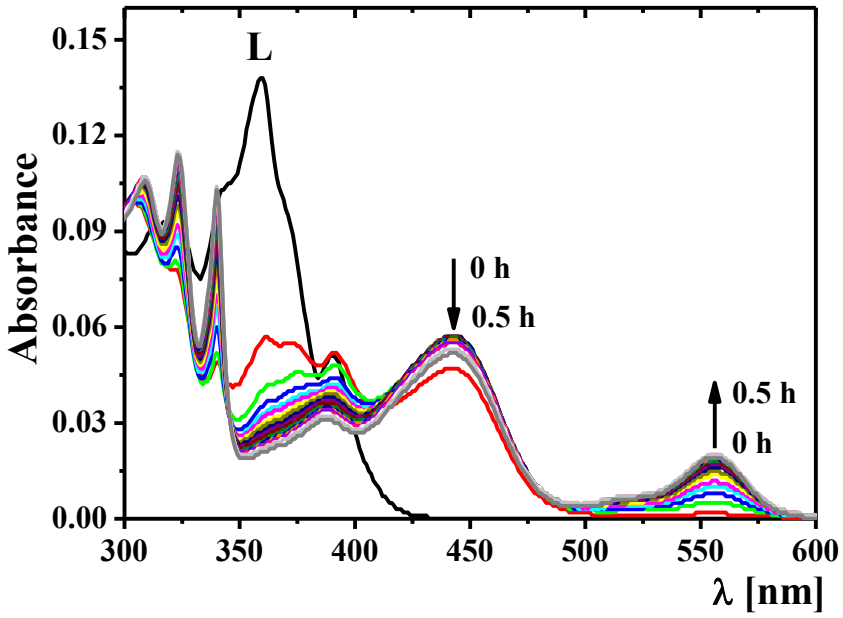

Fig. S11. Changes in the absorbance of **L** (5 μM) with time (from 0 to 0.5 h) in presence of Al^{3+} (100 μM) in HEPES buffer (0.1 M; EtOH: H_2O, 4:1 v/v; pH 7.4) solution.

This journal is © The Royal Society of Chemistry 2013

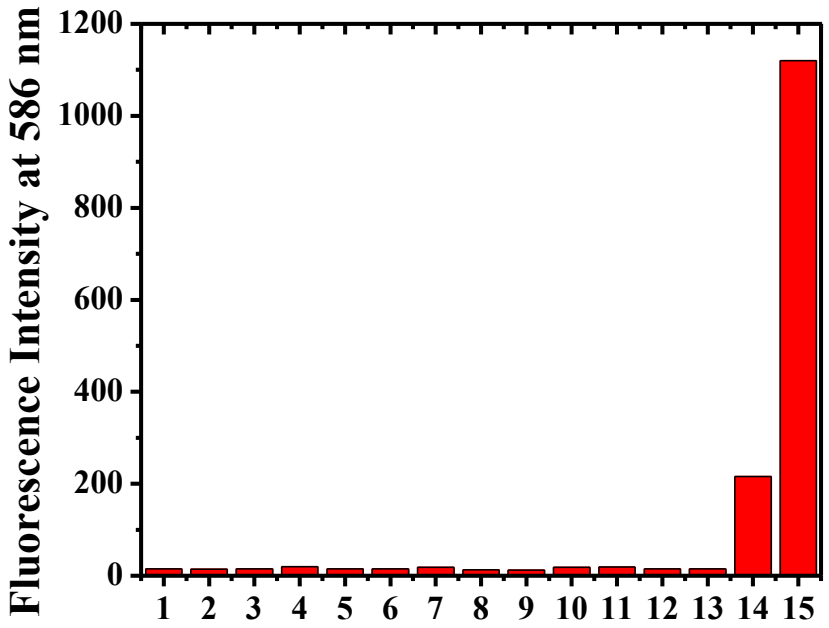

Fig. S12. Plot of the fluorescence intensity of **L** in the presence of different cations in HEPES buffer (0.1 M; EtOH:H_2O, 4:1 v/v; pH 7.4). **L** (10 μM) + M^{n+} (120 μM), where M^{n+} = Na^+ (**1**), K^+ (**2**), Ca^{2+} (**3**), Mg^{2+} (**4**), Mn^{2+} (**5**), Ni^{2+} (**6**), Cr^{3+} (**7**), Fe^{3+} (**8**), Cu^{2+} (**9**), Ag^+ (**10**), Zn^{2+} (**11**), Cd^{2+} (**12**), Pb^{2+} (**13**), Hg^{2+} (**14**), Al^{3+} (**15**). All spectra were recorded after 30 min of mixing of **L** with M^{n+}, λ_{ex} = 400 nm.

This journal is © The Royal Society of Chemistry 2013

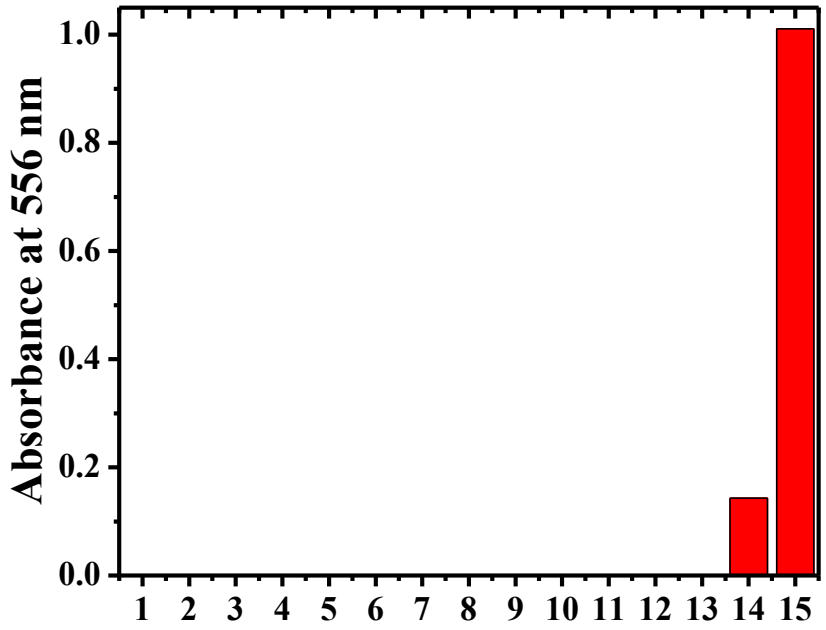

Fig. S13. Plot of absorbance of **L** in the presence of different cations in HEPES buffer (0.1 M; EtOH: H_2O, 4:1 v/v; pH 7.4). **L** (10 μM) + M^{n+} (120 μM), where M^{n+} = Na^+ (**1**), K^+ (**2**), Ca^{2+} (**3**), Mg^{2+} (**4**), Mn^{2+} (**5**), Ni^{2+} (**6**), Cr^{3+} (**7**), Fe^{3+} (**8**), Cu^{2+} (**9**), Ag^+ (**10**), Zn^{2+} (**11**), Cd^{2+} (**12**), Pb^{2+} (**13**), Hg^{2+} (**14**), Al^{3+} (**15**). All spectra were recorded after 30 min of mixing of **L** with M^{n+}.

This journal is © The Royal Society of Chemistry 2013

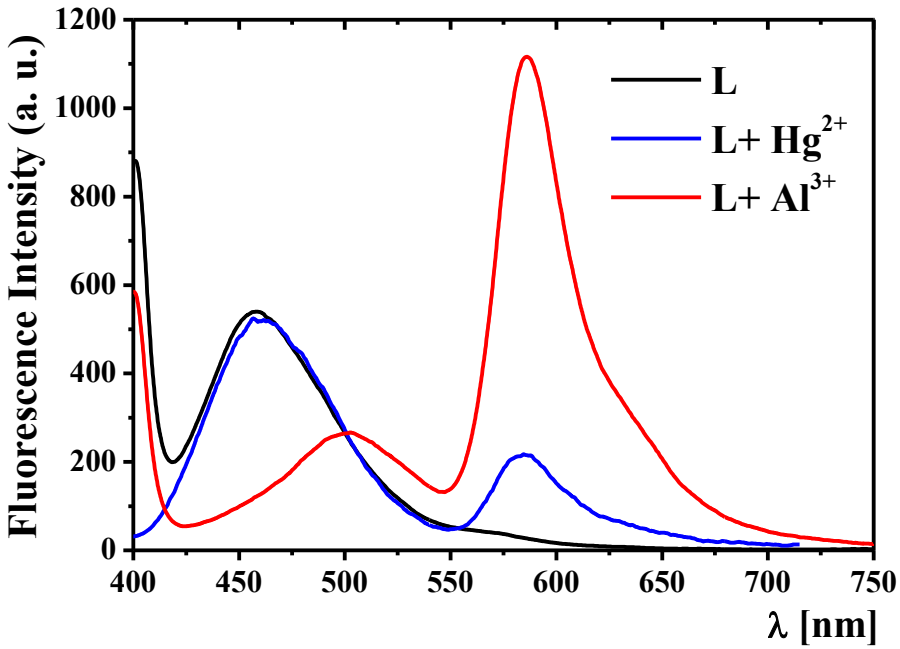

Fig. S14. Plot of the fluorescence intensity of **L** (10 μM) in the presence of Hg^{2+} (120 μM) and Al^{3+} (120 μM) in HEPES buffer (0.1 M; EtOH: H_2O, 4:1 v/v; pH 7.4). All spectra were recorded after 30 min of mixing of **L** with M^{n+}, λ_{ex} = 400 nm.

This journal is © The Royal Society of Chemistry 2013

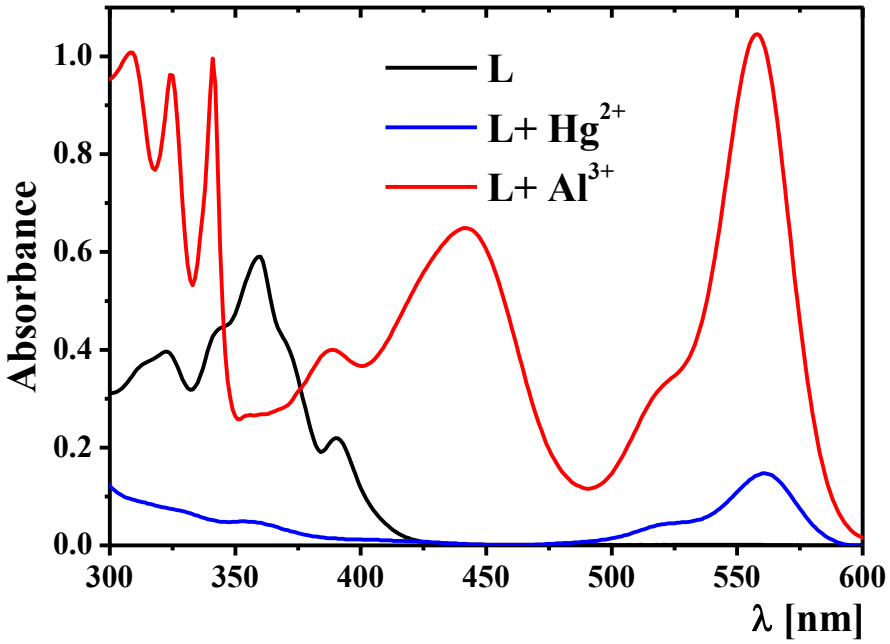

Fig. S15. Plot of absorbance of **L** (10 μM) in the presence of Hg^{2+} (120 μM) and Al^{3+} (120 μM) in HEPES buffer (0.1 M; EtOH: H_2O, 4:1 v/v; pH 7.4). All spectra were recorded after 30 min of mixing of **L** with M^{n+}.

This journal is © The Royal Society of Chemistry 2013

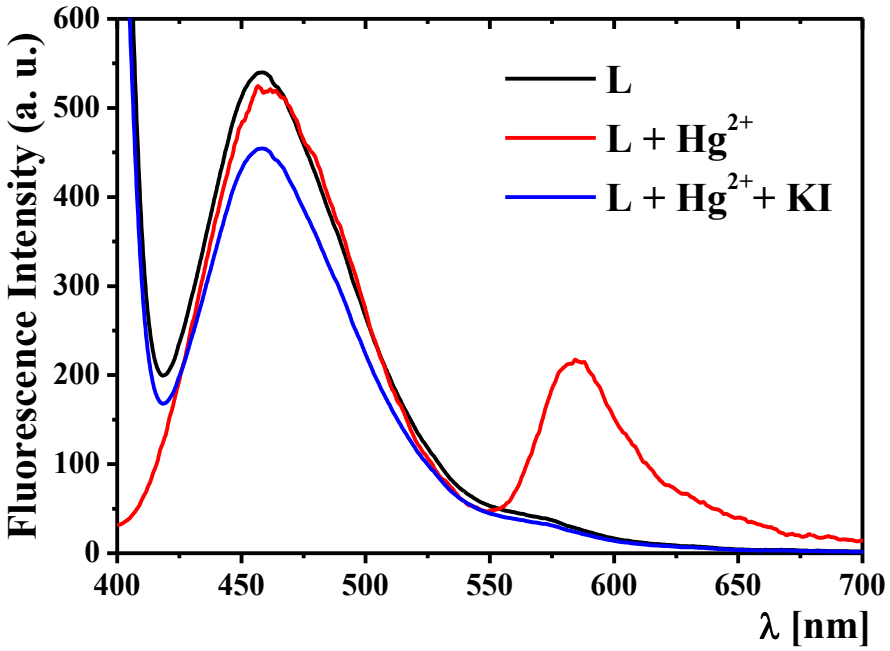

Fig. S16. Effect of Hg^{2+} (120 μM) on the fluorescence spectra of **L** (10 μM) and use of KI (200 μM) to nullify the interference in HEPES buffer (0.1 M; EtOH: H_2O, 4:1 v/v; pH 7.4; λ_{ex} = 400 nm). All spectra were recorded after 30 min of mixing of **L** with Hg^{2+}, λ_{ex} = 400 nm.

This journal is © The Royal Society of Chemistry 2013

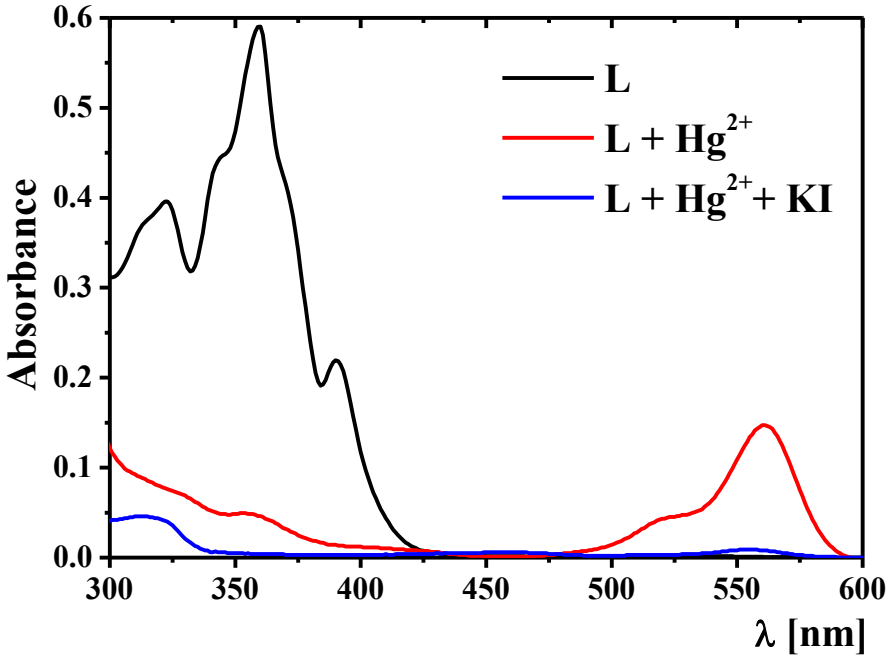

Fig. S17. Effect of Hg^{2+} (120 μM) on absorbance of **L** (10 μM) and use of KI (200 μM) to nullify the interference in HEPES buffer (0.1 M; EtOH: H_2O, 4:1 v/v; pH 7.4; λ_{ex} = 400 nm). All spectra were recorded after 30 min of mixing of **L** with Hg^{2+}.

This journal is © The Royal Society of Chemistry 2013

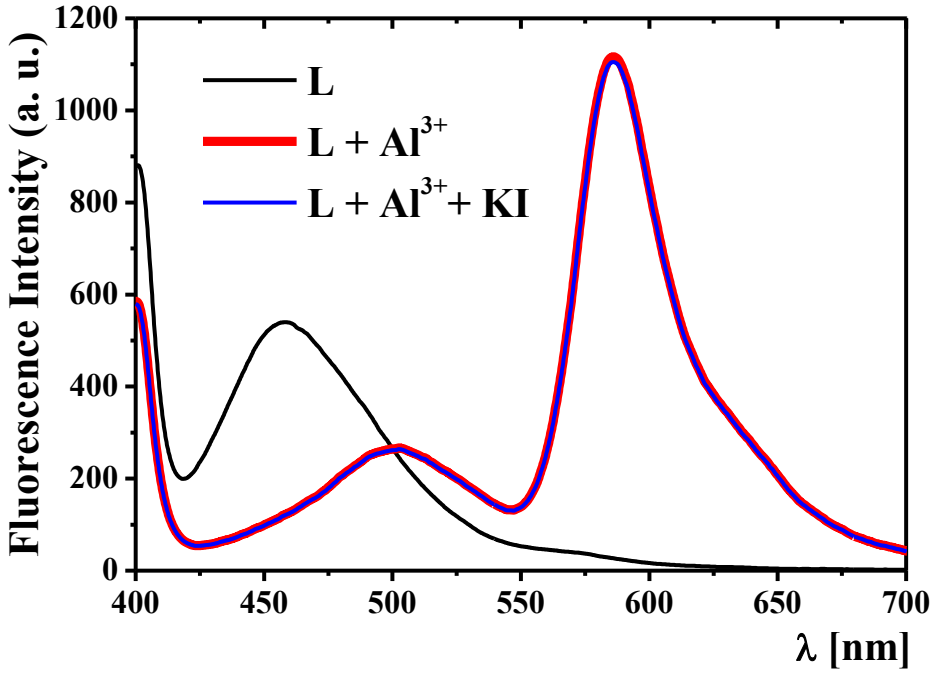

Fig. S18. Effect of Al^{3+} (120 μM) on the fluorescence spectra of **L** (10 μM) with the further addition of KI (200 μM) in HEPES buffer (0.1 M; EtOH: H_2O, 4:1 v/v; pH 7.4). All spectra were recorded after 30 min of mixing of **L** with Al^{3+}, λ_{ex} = 400 nm.

This journal is © The Royal Society of Chemistry 2013

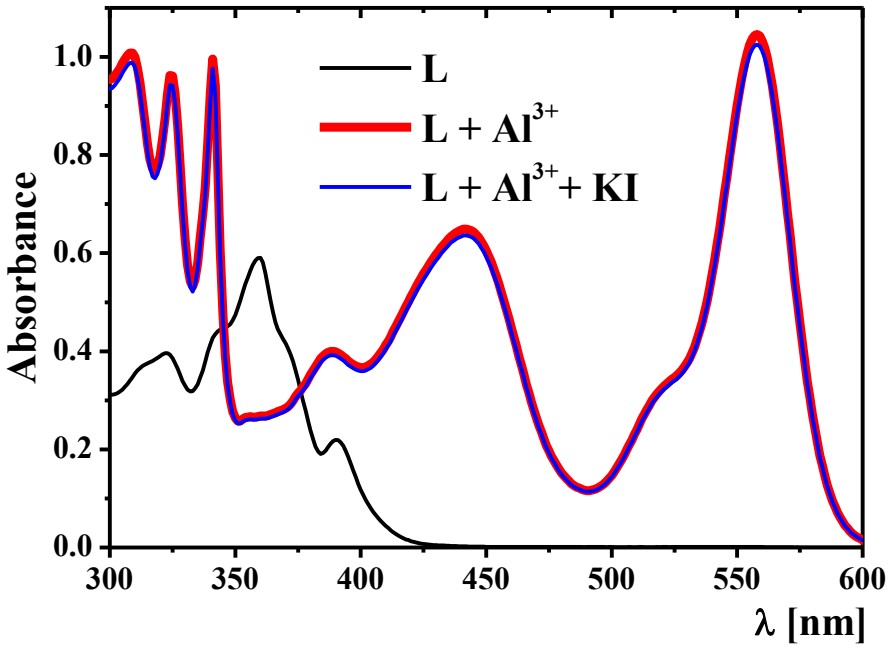

Fig. S19. Effect of Al^{3+} (120 μM) on absorbance of **L** (10 μM) with the further addition of KI (200 μM) in HEPES buffer (0.1 M; EtOH: H_2O, 4:1 v/v; pH 7.4). All spectra were recorded after 30 min of mixing of **L** with Al^{3+}.

This journal is © The Royal Society of Chemistry 2013

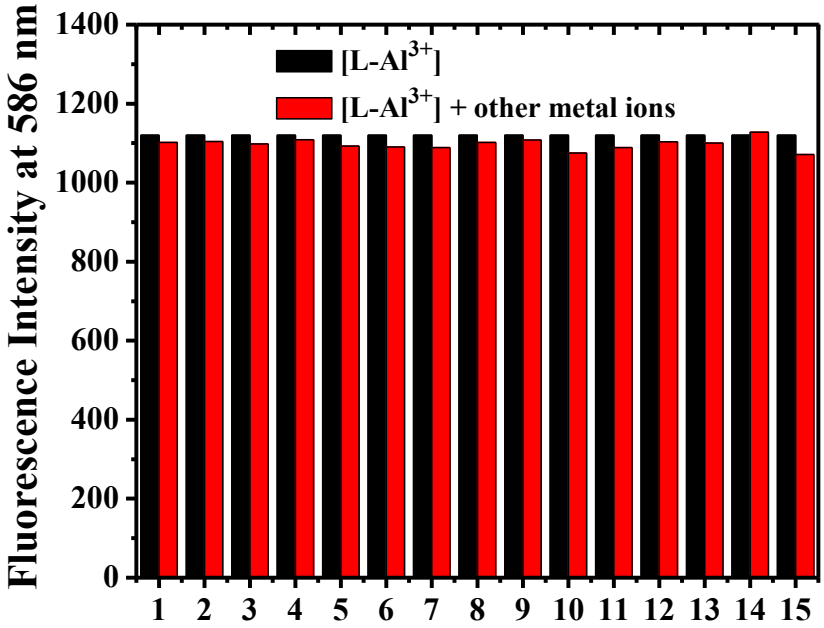

Fig. S20. Plot of the fluorescence intensity of the [**L**–Al^{3+}] system in the presence of different cations in HEPES buffer (0.1 M; EtOH: H_2O, 4:1 v/v; pH 7.4). **L** (10 μM) + Al^{3+} (120 μM) + M^{n+} (200μM), where M^{n+} = Na^+ (**1**), K^+ (**2**), Ca^{2+} (**3**), Mg^{2+} (**4**), Mn^{2+} (**5**), Ni^{2+} (**6**), Cr^{3+} (**7**), Fe^{3+} (**8**), Cu^{2+} (**9**), Co^{2+} (**10**), Ag^+ (**11**), Zn^{2+} (**12**), Cd^{2+} (**13**), Pb^{2+} (**14**), Hg^{2+} (**15**). All spectra were recorded after 30 min of mixing of [**L**–Al^{3+}] with M^{n+}, λ_{ex} = 400 nm.

This journal is © The Royal Society of Chemistry 2013

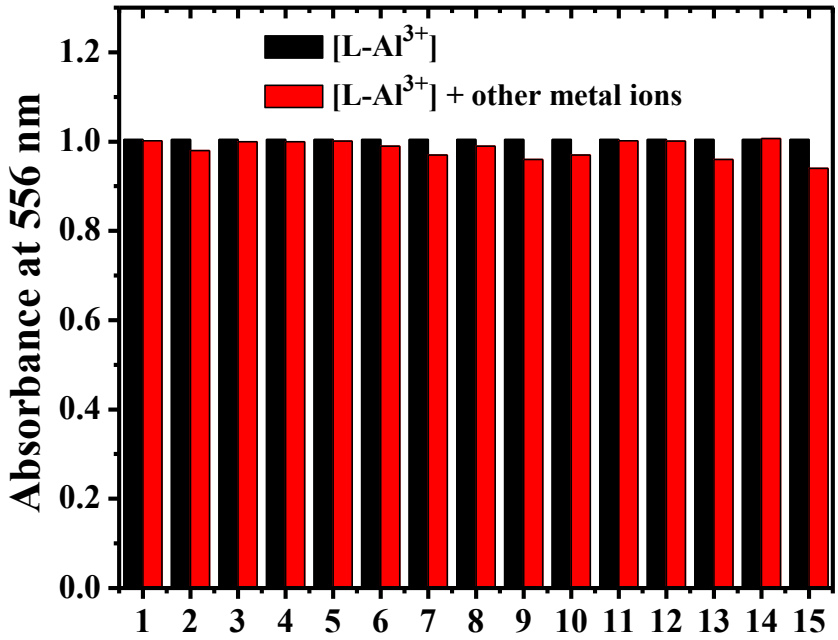

Fig. S21. Plot of absorbance of the [**L**–Al^{3+}] system in the presence of different cations in HEPES buffer (0.1 M; EtOH: H_2O, 4:1 v/v; pH 7.4). **L** (10 μM) + Al^{3+} (120 μM) + M^{n+} (200 μM), where M^{n+} = Na^{+} (**1**), K^{+} (**2**), Ca^{2+} (**3**), Mg^{2+} (**4**), Mn^{2+} (**5**), Ni^{2+} (**6**), Cr^{3+} (**7**), Fe^{3+} (**8**), Cu^{2+} (**9**), Co^{2+} (**10**), Ag^{+} (**11**), Zn^{2+} (**12**), Cd^{2+} (**13**), Pb^{2+} (**14**), Hg^{2+} (**15**). All spectra were recorded after 30 min of mixing of [**L**–Al^{3+}] with M^{n+}.

This journal is © The Royal Society of Chemistry 2013

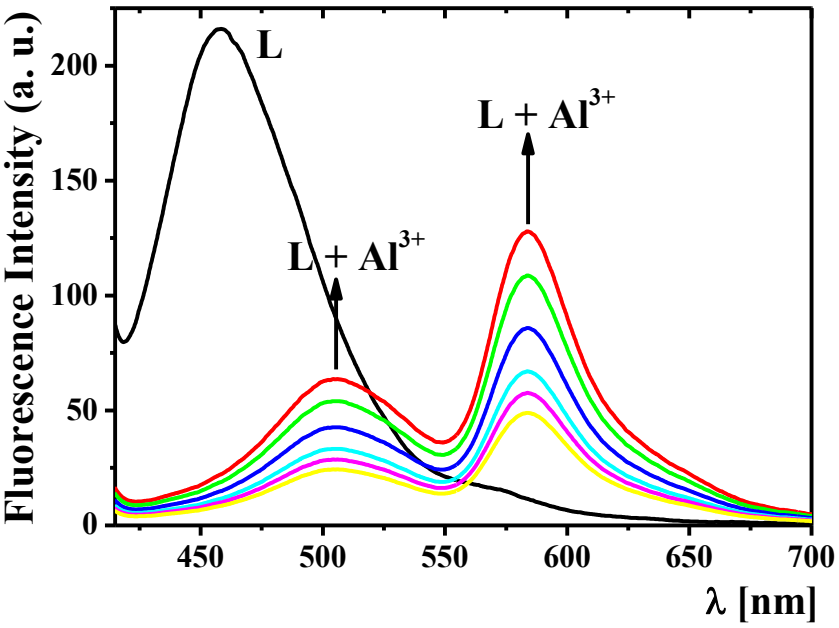

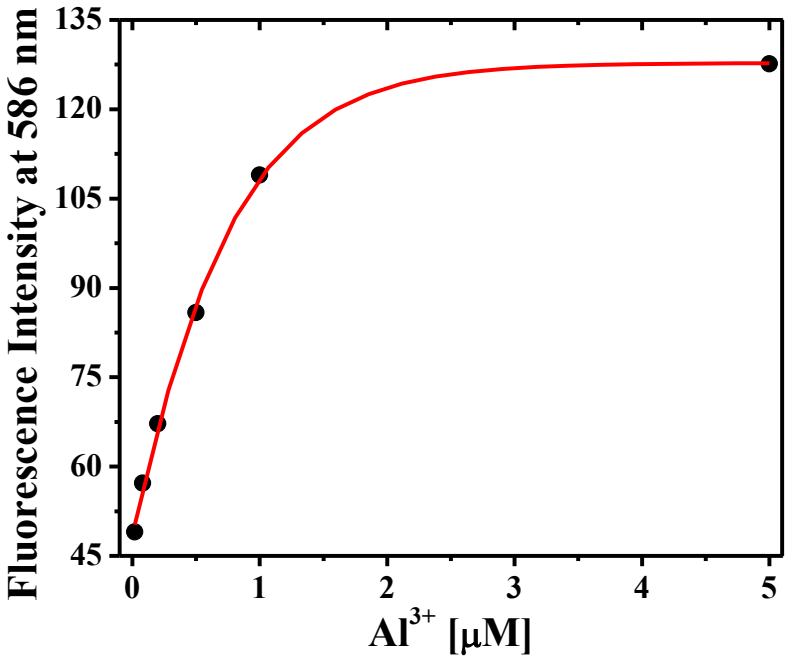

Fig. S22. Changes of the emission intensity of **L** (5 μM) in HEPES buffer (0.1 M; EtOH:H_2O, 4:1 v/v; pH 7.4; λ_{ex} = 400 nm) upon gradual addition of Al^{3+} (0, 0.02, 0.08, 0.2, 0.5, 1.0, 5.0 μM) (top). All spectra are recorded after 30 min of mixing of **L** with Al^{3+}, λ_{ex} = 400 nm. Plot of emission intensity at 586 nm *vs.* concentration of Al^{3+} (0, 0.02, 0.08, 0.2, 0.5, 1.0, 5.0 μM; [**L**] = 5 μM) (bottom).

This journal is © The Royal Society of Chemistry 2013

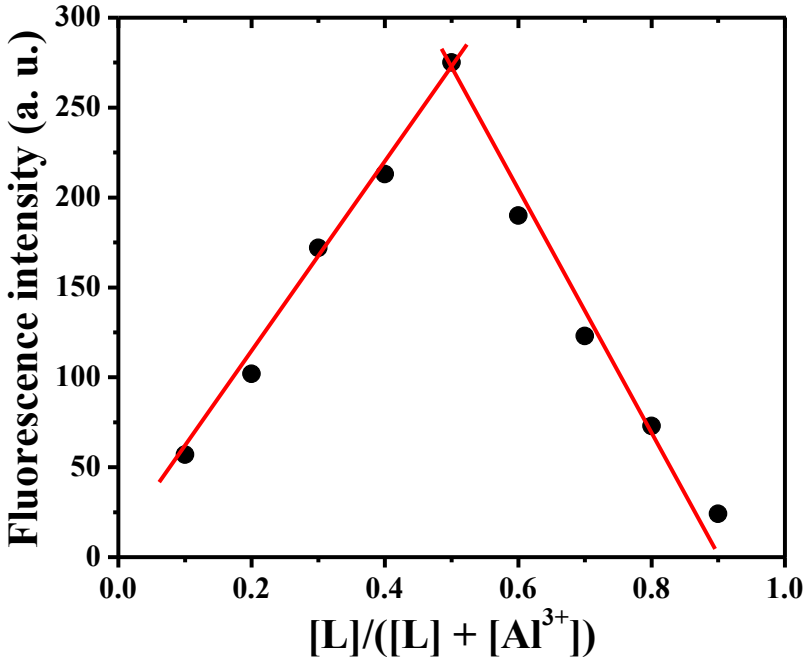

Fig. S23. Job's plot for the determination of stoichiometry of the [**L**–Al^{3+}] system in HEPES buffer (0.1 M; EtOH: H_2O, 4:1 v/v; pH 7.4). Emission intensities at 586 nm are plotted against [**L**]/([**L**] + [Al^{3+}]). All spectra are recorded after 30 min of mixing of **L** with Al^{3+}, λ_{ex} = 400 nm.

This journal is © The Royal Society of Chemistry 2013

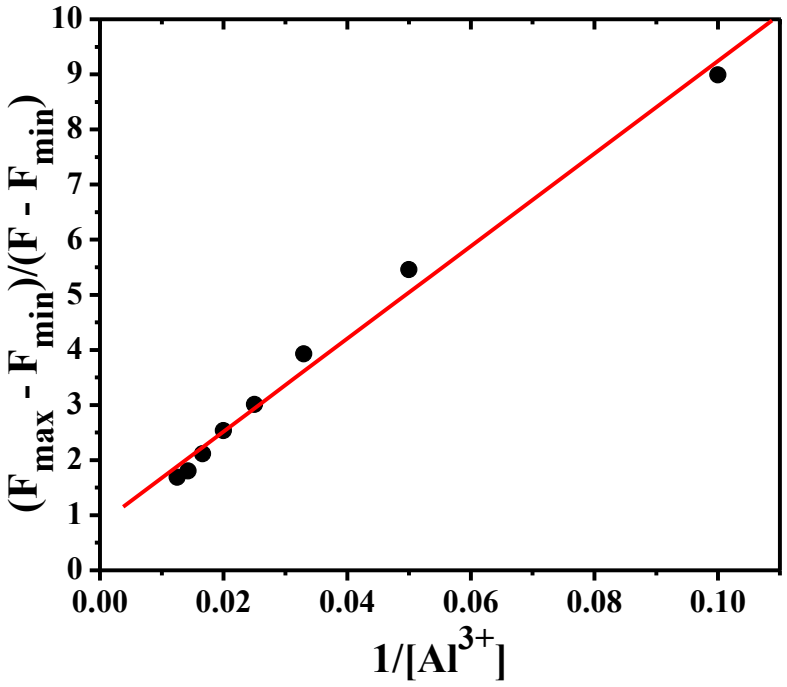

Fig. S24. Determination of the binding constant *K* of **L** for Al^{3+}, where F_{max}, F, and F_{min} are fluorescence intensities of **L** in the presence of Al^{3+} at saturation at 586 nm, fluorescence intensities of free **L** at 455 nm and fluorescence intensities of **L** at any intermediate Al^{3+}concentration at 586 nm, λ_{ex} = 400 nm.

This journal is © The Royal Society of Chemistry 2013

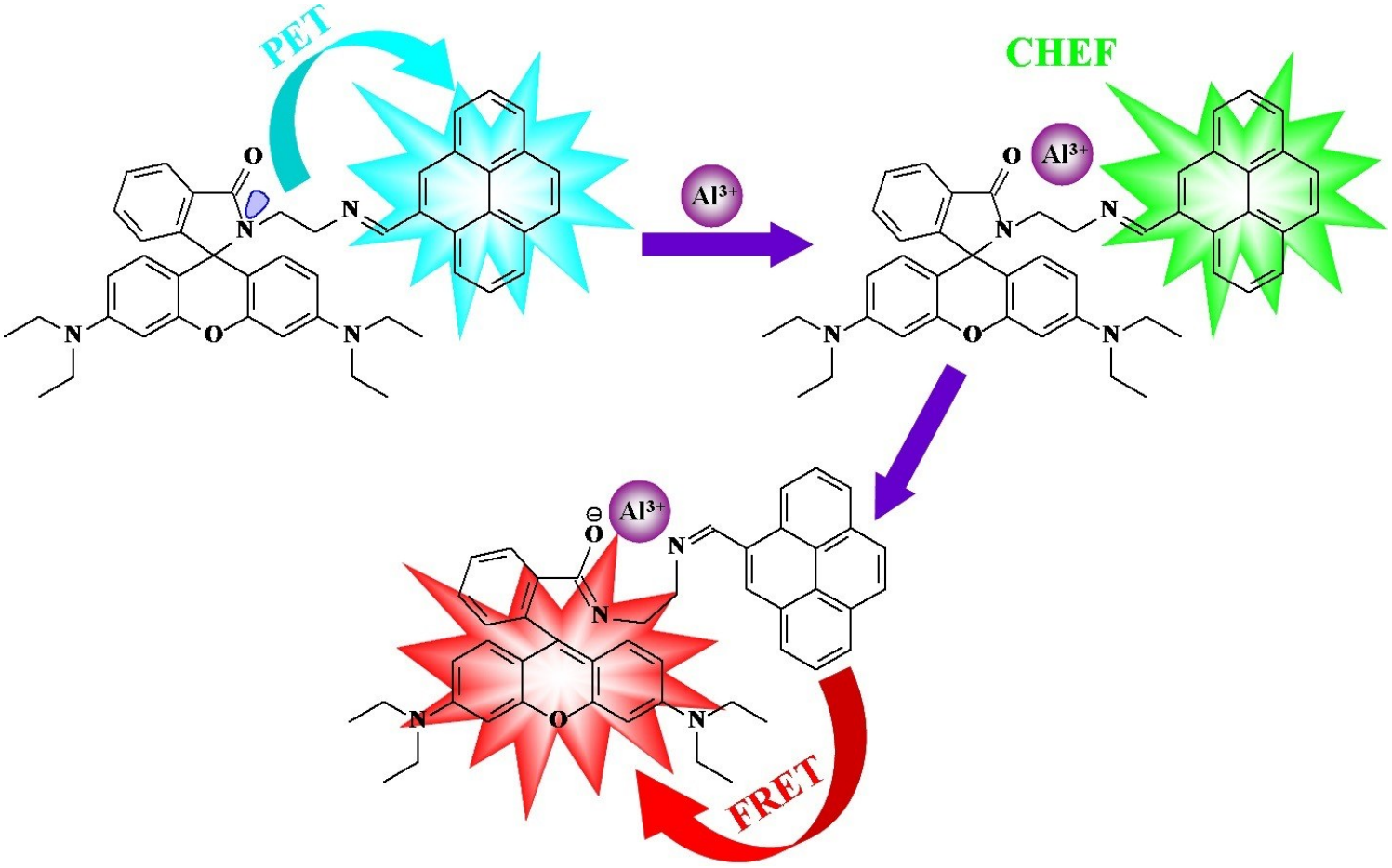

Fig. S25. Proposed Al^{3+} sensing mechanism by **L** through tri-color emission.

This journal is © The Royal Society of Chemistry 2013

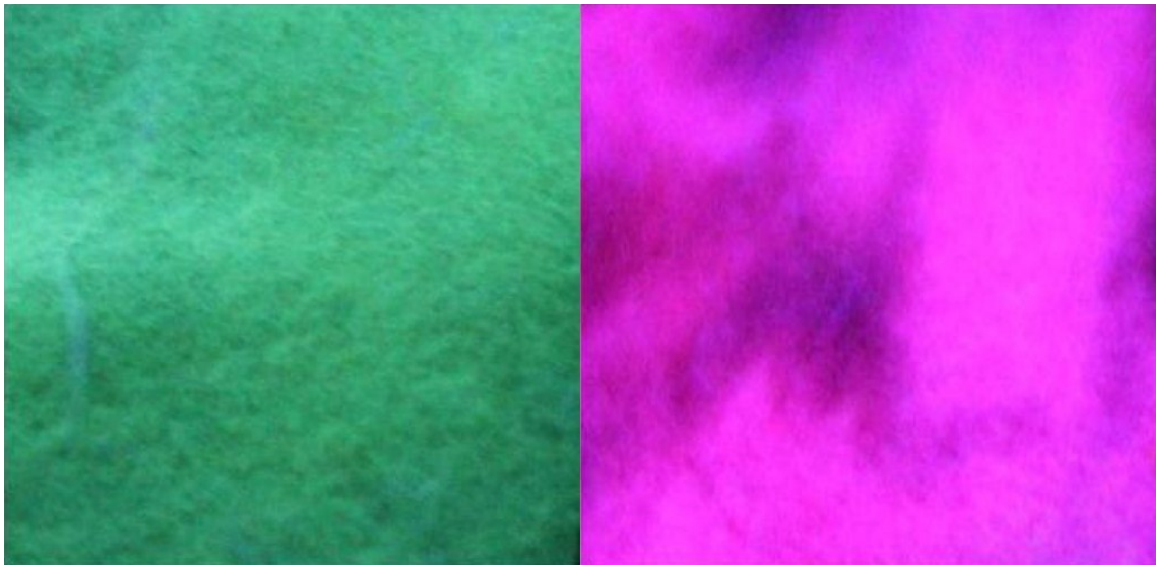

Fig. S26. Time dependent color change of **L** (10 μM) soaked paper in the presence of Al^{3+} (50 μM) under a hand held UV lamp: after 5 min (left) and after 30 min (right).

This journal is © The Royal Society of Chemistry 2013

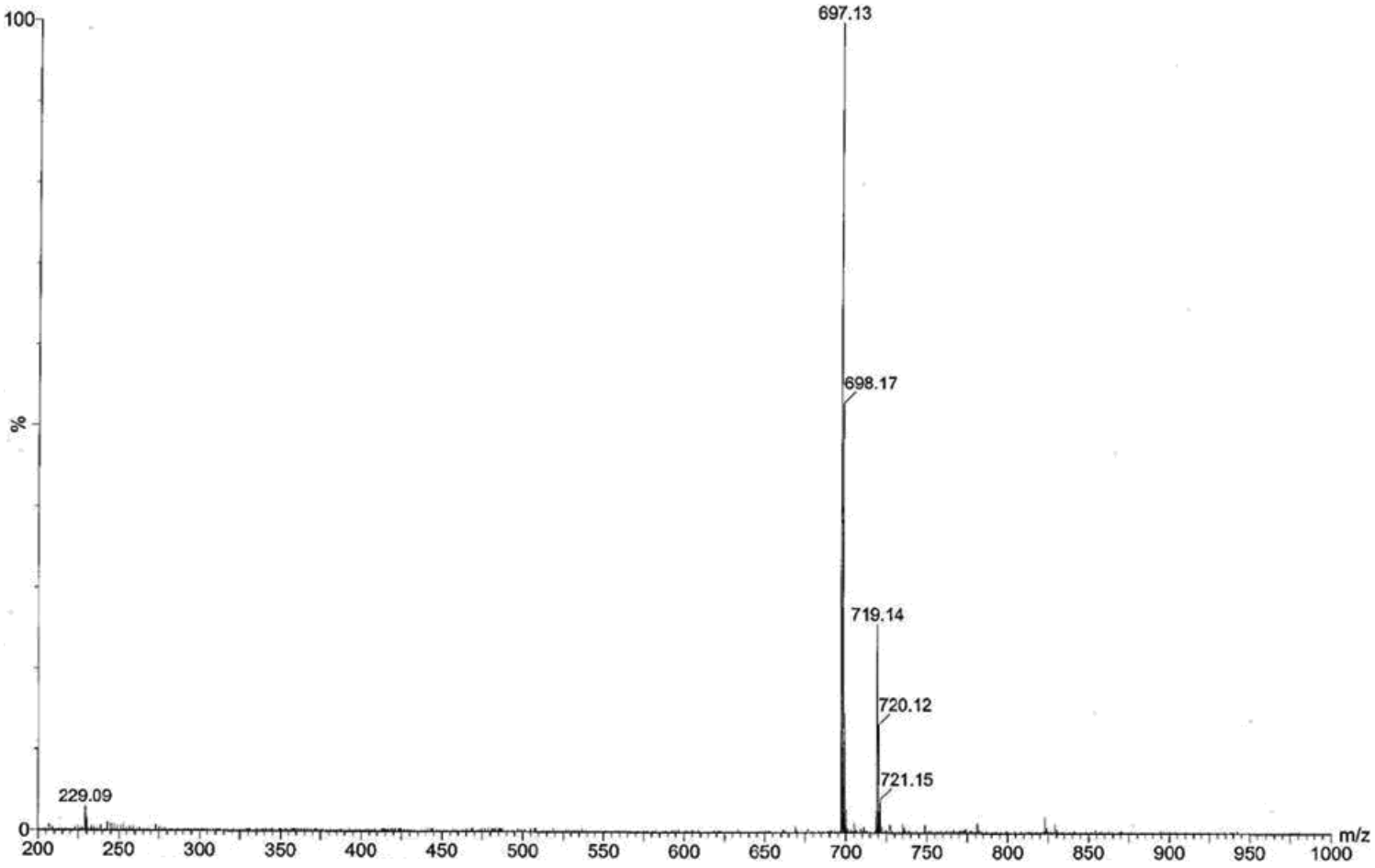

Fig. S27. QTOF-MS spectrum of **L** in MeOH.

This journal is © The Royal Society of Chemistry 2013

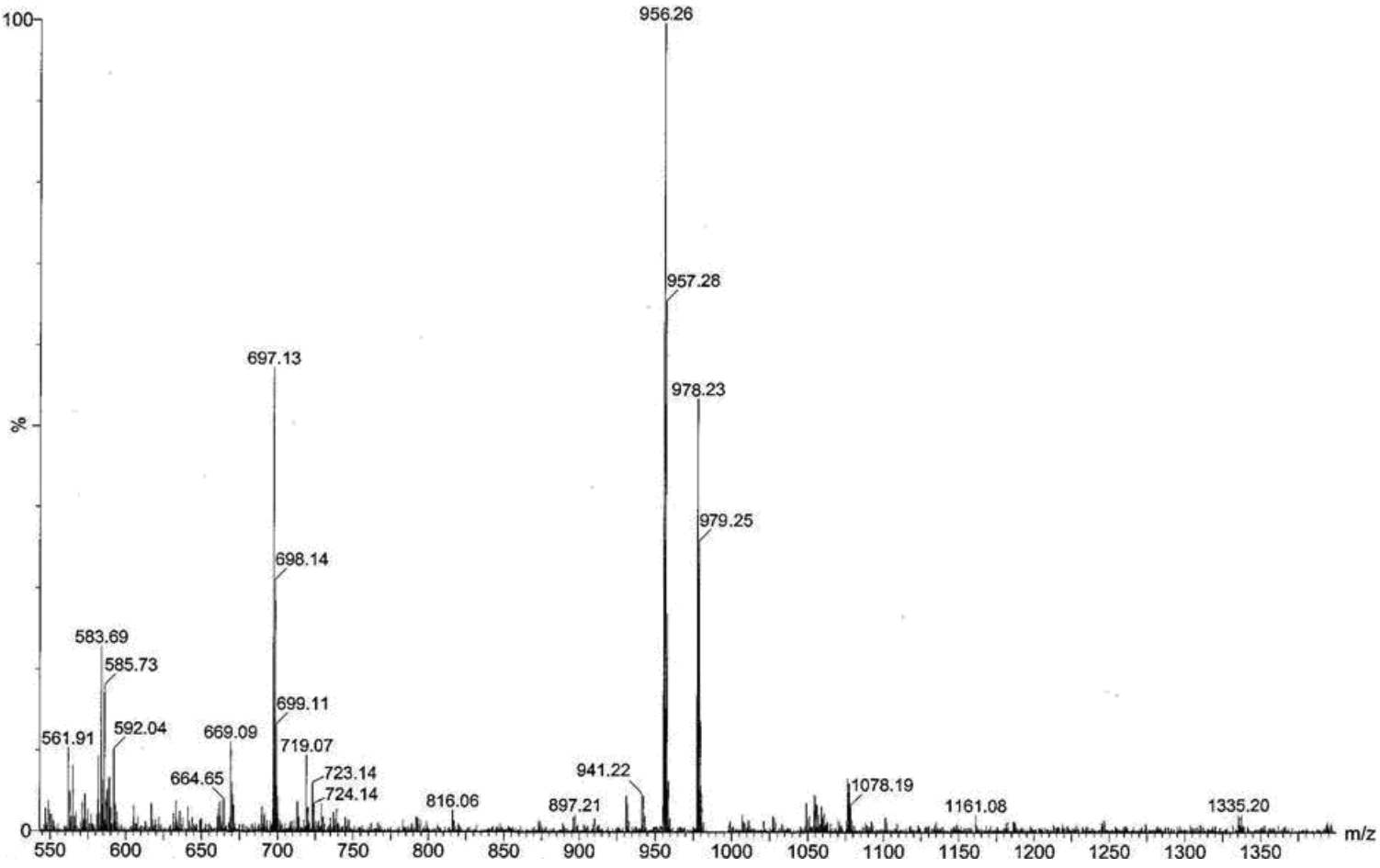

Fig. S28. QTOF-MS spectrum of the [**L**–Al^{3+}] system in MeOH.

This journal is © The Royal Society of Chemistry 2013

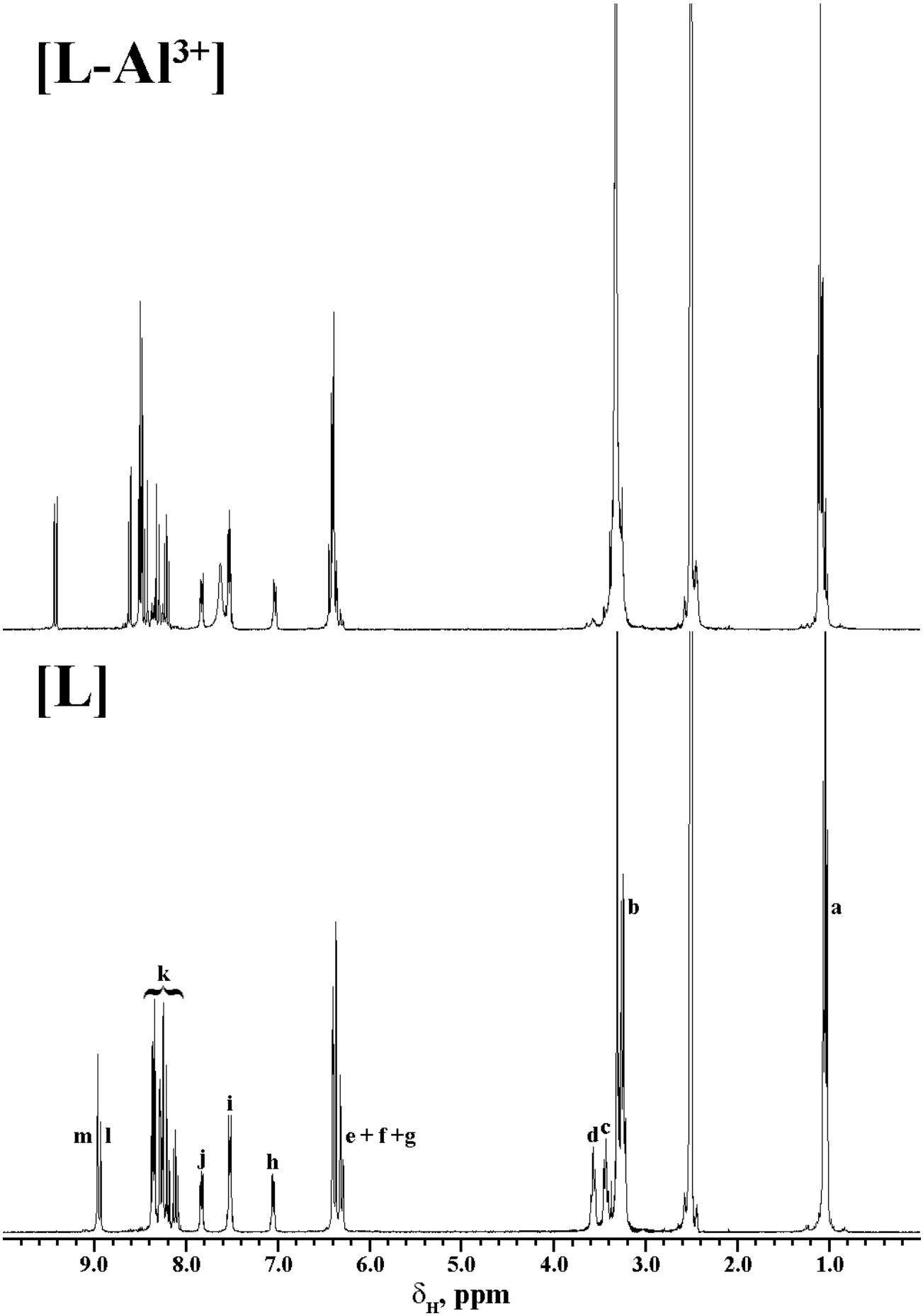

Fig. S29. ^{1}H NMR spectra of **L** before and after 0.5 h of addition of 1 equivalent of $Al(NO_3)_3 \cdot 9H_2O$ in DMSO-d_6 (for protons assignment see Scheme S1).

This journal is © The Royal Society of Chemistry 2013

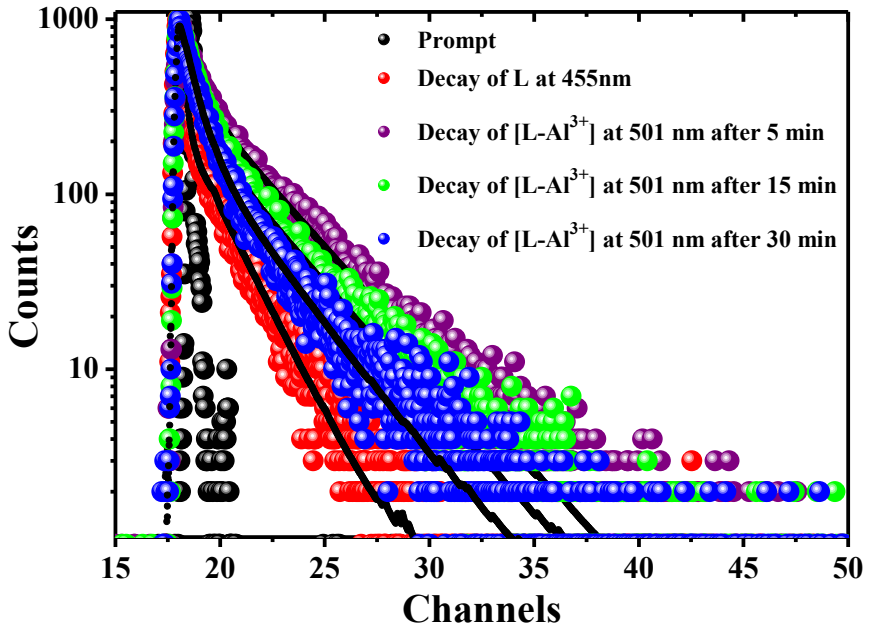

Fig. S30. Fluorescence lifetime decay of **L** at 455 nm and [**L**–Al^{3+}] at 501 nm.

This journal is © The Royal Society of Chemistry 2013

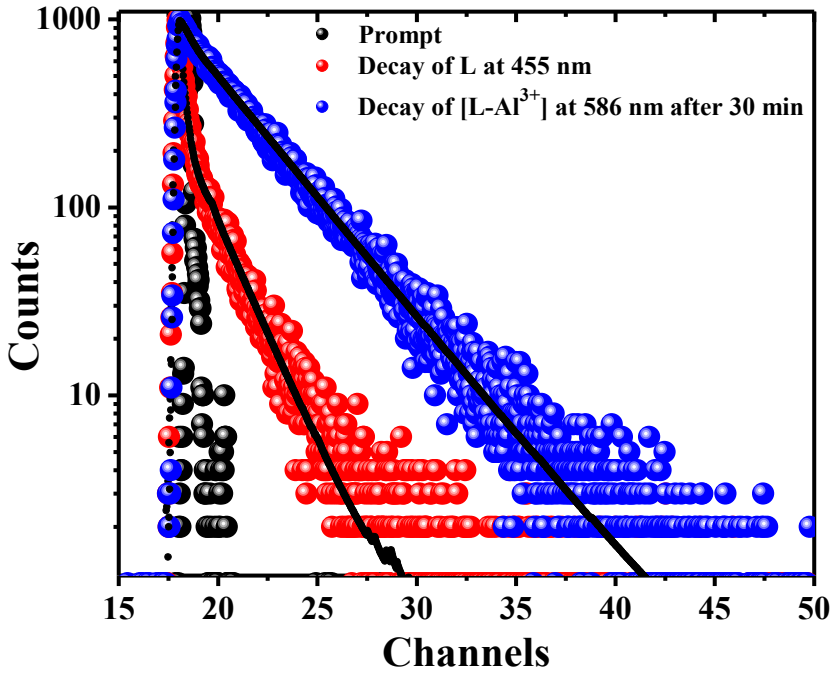

Fig. S31. Fluorescence lifetime decay of **L** at 455 nm and [**L**–Al^{3+}] at 586 nm.

This journal is © The Royal Society of Chemistry 2013

Table S1. Selected bond lengths (Å) and bond angles (°) for **L**

Bond lengths

O(1)–C(1)	1.235(4)	C(5)–C(41)	1.462(5)	C(25)–C(26)	1.370(5)	C(43)–C(44)	1.405(4)
O(2)–C(22)	1.378(4)	C(6)–C(31)	1.518(5)	C(27)–C(28)	1.510(6)	C(43)–C(51)	1.447(5)
O(2)–C(32)	1.384(4)	C(6)–C(21)	1.520(5)	C(29)–C(30)	1.490(5)	C(44)–C(45)	1.400(5)
N(1)–C(1)	1.355(4)	C(6)–C(11)	1.524(4)	C(31)–C(32)	1.376(4)	C(44)–C(49)	1.432(5)
N(1)–C(2)	1.448(4)	C(11)–C(12)	1.371(5)	C(31)–C(36)	1.391(5)	C(45)–C(46)	1.374(4)
N(1)–C(6)	1.496(4)	C(11)–C(16)	1.382(5)	C(32)–C(33)	1.376(5)	C(47)–C(48)	1.356(5)
N(2)–C(24)	1.382(5)	C(12)–C(13)	1.383(5)	C(33)–C(34)	1.385(5)	C(48)–C(52)	1.426(5)
N(2)–C(27)	1.479(5)	C(13)–C(14)	1.388(5)	C(34)–C(35)	1.408(5)	C(49)–C(50)	1.336(5)
N(2)–C(29)	1.494(5)	C(14)–C(15)	1.379(6)	C(35)–C(36)	1.358(5)	C(50)–C(56)	1.421(5)
N(3)–C(34)	1.381(4)	C(15)–C(16)	1.389(5)	C(37)–C(38)	1.456(6)	C(51)–C(52)	1.409(4)
N(3)–C(39)	1.462(5)	C(21)–C(22)	1.372(5)	C(39)–C(40)	1.514(5)	C(51)–C(56)	1.427(4)
N(3)–C(37)	1.490(5)	C(21)–C(26)	1.407(5)	C(41)–C(46)	1.388(4)	C(52)–C(53)	1.402(5)
N(4)–C(5)	1.259(4)	C(22)–C(23)	1.387(5)	C(41)–C(42)	1.413(5)	C(53)–C(54)	1.388(5)
N(4)–C(3)	1.467(4)	C(23)–C(24)	1.404(5)	C(42)–C(43)	1.420(4)	C(54)–C(55)	1.365(5)
C(1)–C(12)	1.479(5)	C(24)–C(25)	1.403(5)	C(42)–C(47)	1.442(4)	C(55)–C(56)	1.405(5)
C(2)–C(3)	1.519(5)						

Bond angles

C(22)–O(2)–C(32)	118.6(3)	C(12)–C(11)–C(16)	121.2(3)	C(30)–C(29)–N(2)	112.2(3)	C(42)–C(43)–C(51)	119.5(3)
C(1)–N(1)–C(2)	121.8(3)	C(12)–C(11)–C(6)	110.9(3)	C(32)–C(31)–C(36)	115.1(3)	C(45)–C(44)–C(43)	118.6(3)
C(1)–N(1)–C(6)	114.7(3)	C(16)–C(11)–C(6)	127.9(3)	C(32)–C(31)–C(6)	122.7(3)	C(45)–C(44)–C(49)	122.8(3)
C(2)–N(1)–C(6)	123.3(3)	C(11)–C(12)–C(13)	121.8(3)	C(36)–C(31)–C(6)	122.2(3)	C(43)–C(44)–C(49)	118.6(3)
C(24)–N(2)–C(27)	122.6(3)	C(11)–C(12)–C(1)	109.2(3)	C(33)–C(32)–C(31)	123.5(3)	C(46)–C(45)–C(44)	120.8(3)
C(24)–N(2)–C(29)	119.1(3)	C(13)–C(12)–C(1)	129.1(4)	C(33)–C(32)–O(2)	113.7(3)	C(45)–C(46)–C(41)	121.5(3)
C(27)–N(2)–C(29)	114.7(3)	C(12)–C(13)–C(14)	117.5(4)	C(31)–C(32)–O(2)	122.9(3)	C(48)–C(47)–C(42)	121.9(3)
C(34)–N(3)–C(39)	120.8(3)	C(15)–C(14)–C(13)	120.7(4)	C(32)–C(33)–C(34)	120.6(3)	C(47)–C(48)–C(52)	121.3(3)
C(34)–N(3)–C(37)	121.8(3)	C(14)–C(15)–C(16)	121.6(4)	N(3)–C(34)–C(33)	120.5(3)	C(50)–C(49)–C(44)	122.4(3)
C(39)–N(3)–C(37)	116.6(3)	C(11)–C(16)–C(15)	117.3(4)	N(3)–C(34)–C(35)	122.6(3)	C(49)–C(50)–C(56)	121.3(3)
C(5)–N(4)–C(3)	116.8(3)	C(22)–C(21)–C(26)	114.8(3)	C(33)–C(34)–C(35)	116.8(3)	C(52)–C(51)–C(56)	120.2(3)
O(1)–C(1)–N(1)	125.4(3)	C(22)–C(21)–C(6)	122.7(3)	C(36)–C(35)–C(34)	120.7(3)	C(52)–C(51)–C(43)	120.4(3)
O(1)–C(1)–C(12)	128.7(3)	C(26)–C(21)–C(6)	122.6(3)	C(35)–C(36)–C(31)	123.2(3)	C(56)–C(51)–C(43)	119.4(3)
N(1)–C(1)–C(12)	105.9(3)	C(21)–C(22)–O(2)	123.2(3)	C(38)–C(37)–N(3)	110.6(4)	C(53)–C(52)–C(51)	119.3(3)
N(1)–C(2)–C(3)	110.8(3)	C(21)–C(22)–C(23)	124.1(3)	N(3)–C(39)–C(40)	116.8(4)	C(53)–C(52)–C(48)	121.9(3)
N(4)–C(3)–C(2)	109.2(3)	O(2)–C(22)–C(23)	112.7(3)	C(46)–C(41)–C(42)	119.6(3)	C(51)–C(52)–C(48)	118.8(3)
N(4)–C(5)–C(41)	122.4(3)	C(22)–C(23)–C(24)	120.6(4)	C(46)–C(41)–C(5)	119.3(3)	C(54)–C(53)–C(52)	119.6(4)
N(1)–C(6)–C(31)	110.7(3)	N(2)–C(24)–C(25)	123.6(4)	C(42)–C(41)–C(5)	121.1(3)	C(55)–C(54)–C(53)	122.1(4)
N(1)–C(6)–C(21)	112.8(3)	N(2)–C(24)–C(23)	120.6(4)	C(41)–C(42)–C(43)	118.5(3)	C(54)–C(55)–C(56)	120.3(4)
C(31)–C(6)–C(21)	109.9(3)	C(25)–C(24)–C(23)	115.8(4)	C(41)–C(42)–C(47)	123.4(3)	C(55)–C(56)–C(50)	122.7(3)
N(1)–C(6)–C(11)	99.3(3)	C(26)–C(25)–C(24)	122.0(4)	C(43)–C(42)–C(47)	118.1(3)	C(55)–C(56)–C(51)	118.6(3)

C(31)–C(6)–C(11)	112.2(3)	C(25)–C(26)–C(21)	122.6(4)	C(44)–C(43)–C(42)	120.9(3)	C(50)–C(56)–C(51)	118.8(3)
C(21)–C(6)–C(11)	111.7(3)	N(2)–C(27)–C(28)	112.7(3)	C(44)–C(43)–C(51)	119.6(3)		

Table S2. Chemical shifts of protons (δ, ppm) in the ^{1}H NMR spectra of **L** before and after addition of 1 equivalent of $Al(NO_3)_3 \cdot 9H_2O$ in DMSO-d_6 (protons a labeled as given in Scheme 1).

	a	**b**	**c**	**d**	**e**	**f**	**g**	**h**	**i**	**j**	**k**	**l**	**m**
L	1.04	3.26	3.43	3.57	6.26–6.44			6.99–7.11	7.45–7.58	7.78–7.88	8.06–8.45	8.93	8.96
[**L**–Al^{3+}]	1.09		3.20–3.40		6.30–6.46			6.99–7.09	7.47–7.56, 7.63[a]	7.78–7.89	8.16–8.67	9.41	9.44

[a] Original signal splitted into two parts.

Table S3. Fluorescence life time decay parameters of **L** and its Al^{3+} complex

	B_1	**τ_1 (ns)**	**B_2**	**τ_2 (ns)**	**$\langle\tau_2\rangle$ (ns)**
L at 455 nm	0.211	0.185	0.028	1.80	0.3788
[**L**–Al^{3+}] at 501 nm after 5 min	0.092	5.930	0.046	3.249	1.484
[**L**–Al^{3+}] at 501 nm after 15 min	0.107	0.662	0.03	3.064	1.219
[**L**–Al^{3+}] at 501 nm after 30 min	0.113	0.062	0.026	2.71	1.010
[**L**–Al^{3+}] at 586 nm after 30 min	0.037	0.617	0.094	3.411	2.611